Published in final edited form as:
Acta Biomater. 2017 October 01; 61: 41–53. doi:10.1016/j.actbio.2017.08.005.

The bio in the ink: cartilage regeneration with bioprintable hydrogels and articular cartilage-derived progenitor cells

Riccardo Levato[a], **William R. Webb**[b], **Iris A. Otto**[a,c], **Anneloes Mensinga**[a], **Yadan Zhang**[b], **Mattie van Rijen**[a], **René van Weeren**[d], **Ilyas M. Khan**[b], **Jos Malda**[a,d,*]

[a]Department of Orthopaedics, University Medical Center Utrecht, PO Box 85500, 3508 GA Utrecht, The Netherlands [b]Center for Nanohealth, Swansea University Medical School, Wales, United Kingdom [c]Department of Plastic and Reconstructive Surgery, University Medical Center Utrecht, Utrecht, The Netherlands [d]Department of Equine Sciences, Faculty of Veterinary Medicine, Utrecht University, Utrecht, The Netherlands

Abstract

Cell-laden hydrogels are the primary building blocks for bioprinting, and, also termed bioinks, are the foundations for creating structures that can potentially recapitulate the architecture of articular cartilage. To be functional, hydrogel constructs need to unlock the regenerative capacity of encapsulated cells. The recent identification of multipotent articular cartilage-resident chondroprogenitor cells (ACPCs), which share important traits with adult stem cells, represents a new opportunity for cartilage regeneration. However, little is known about the suitability of ACPCs for tissue engineering, especially in combination with biomaterials. This study aimed to investigate the potential of ACPCs in hydrogels for cartilage regeneration and biofabrication, and to evaluate their ability for zone-specific matrix production. Gelatin methacryloyl (gelMA)-based hydrogels were used to culture ACPCs, bone marrow mesenchymal stromal cells (MSCs) and chondrocytes, and as bioinks for printing. Our data shows ACPCs outperformed chondrocytes in terms of neo-cartilage production and unlike MSCs, ACPCs had the lowest gene expression levels of hypertrophy marker collagen type X, and the highest expression of PRG4, a key factor in joint lubrication. Co-cultures of the cell types in multi-compartment hydrogels allowed generating constructs with a layered distribution of collagens and glycosaminoglycans. By combining ACPC- and MSC-laden bioinks, a bioprinted model of articular cartilage was generated, consisting of defined superficial and deep regions, each with distinct cellular and extracellular matrix composition. Taken together, these results provide important information for the use of ACPC-laden hydrogels in regenerative medicine, and pave the way to the biofabrication of 3 D constructs with multiple cell types for cartilage regeneration or *in vitro* tissue models.

*Corresponding author at: Department of Orthopaedics, University Medical Center Utrecht, PO Box 85500, 3508 GA Utrecht, The Netherlands. j.malda@umcutrecht.nl (J. Malda).

Conflict of interest
The authors declare no conflicts of interest.

Author contributions
R.L., W.R.W, R.vW., I.M.K., J.M. designed the experiments; R.L., W.R.W., I.A.O. performed the experiments; A.M., M.vR., provided technical support and performed gene expression and histological analysis; R.L. W.R.W., R.vW., Y.Z., I.M.K., J.M. analyzed data; R.L. wrote the paper with inputs from all authors. All authors have approved the final article.

Europe PMC Funders Author Manuscripts

Keywords

Hydrogel; Chondroprogenitor cells; Biofabrication; Cartilage regeneration; Stem cells; Co-culture

1 Introduction

Articular cartilage defects do not heal spontaneously and are prone to progress towards osteoarthritis, eventually resulting in impaired joint function, disability and a reduced quality of life [1]. Therapies involving the delivery of cells, including autologous chondrocyte implantation have substantially improved the outcome of treatments of such defects [2], but unfortunately often result in a low-performance repair tissue, which only delays the onset of degeneration and osteoarthritis [3].

In the quest for therapies that enhance cartilage healing, hydrogel-based constructs are particularly appealing for regenerative medicine, as they allow encapsulation of cells in a highly hydrated environment, analogous to that of native cartilage [4]. Moreover, cell-laden hydrogels can be used as bioinks, which are the building blocks of many biofabrication strategies [5]. Biofabrication allow the coordinated deposition of multiple cells and materials in a layer-by-layer fashion, enabling three-dimensional (3D) bioprinting of patient-specific and anatomically-shaped grafts [6]. Bioprinting also allows for the possibility of mimicking tissuespecific architecture such as the zonal and depth-dependent structure of articular cartilage [7]and also recreating the transition and interface between contiguous tissues [8].

While biofabrication holds the promise of introducing a new generation of regenerative therapies for cartilage [9], simply recapitulating the native structural and cellular composition during the printing process is only the first step of many. Regeneration is driven by the encapsulated cells (and, upon implantation, by the interplay with the host biomechanical and biochemical environment) and occurs over time, after the initial bioprinting step. Thus, in the design of hydrogels, and consequently bioinks, harnessing the potential of regeneration-competent cells is paramount. Nevertheless, the optimal cell source to be incorporated for cartilagebased cell therapies and tissue engineering is still subject of ongoing debate [10].

Chondrocytes are known to recover their ability to deposit cartilage-like matrix when cultured in a 3D hydrogel environment [11], but steadily lose their re-differentiation capacity after a few population doublings limiting their usefulness for cell therapy and tissue engineering of larger defects. To bypass this limitation, multipotent progenitor cells, such as mesenchymal stromal cells (MSC) derived from the synovium [12], umbilical cord [13], bone marrow [14]or adipose tissue [15]have also been applied to synthesize new cartilage in hydrogel matrices. However, while MSCs have been used with beneficial effects to the level of clinical trial [16], their tendency to undergo hypertrophic differentiation and trigger endochondral ossification remains a major concern [17].

Recently, the identification and characterization of a population of a resident, cartilage-specific, multipotent progenitor cells has opened new avenues for cartilage repair [18,19]. Articular cartilage-derived progenitor cells (ACPCs) are found both in young and adult

cartilage and make up about 0.1-1% of cartilage cell content. They are mainly located in the superficial zone of articular cartilage and express high levels of integrin alpha5, and thus can be enriched by differential adhesion to fibronectin, as no unique marker has been identified yet [18,20]. To date, ACPCs have been isolated from different species, including of human, equine and bovine.

ACPCs are sometimes referred to as cartilage progenitor/stem cells [21]or simply chondroprogenitors [22], although the latter term can create confusion, since it is also often used to describe any progenitor cell which has been driven towards chondrogenic differentiation, including MSCs, synovial fluid or synovial membrane-derived cells and epiphiseal progenitors [23,24]. Much like MSCs, ACPCs are capable of *in vitro* self-renewal, and can be expanded to more than 60 population doublings while maintaining their potential to differentiate towards osteo-, chondro- and adipogenic lineages [18]. Interestingly, ACPCs play an important role in cartilage development [25], maturation [26], repair upon injury and response to osteoarthritic changes in the joint [21,27]. Moreover, unlike MSCs, ACPCs appear to show low or no expression of RUNX2, the master transcription factor for chondrocyte terminal differentiation and subsequent formation of calcified tissue [28]. This resistance to hypertrophy and the consistent production of hyaline-like cartilage from ACPC is maintained also during dynamic culture under multiaxial mechanical loading [29]. Additionally, ACPCs have been proposed as cell sources for autologous transplantation in cartilage in equine models [30], and even in a pilot clinical trial in humans with encouraging results [31]. Despite promising characteristics for cell and tissue therapies, the potential of ACPCs for tissue engineering is unexplored, in particular the behavior of ACPCs in 3D culture and biomaterial-driven tissue regeneration remains to be studied. Indeed, ACPCs have received limited attention in the biomaterials community as cell source for producing cartilage constructs, and only a few studies have highlighted their utilization in combination with scaffolds, even though adult, tissue-specific progenitor cells have been important resources for the regeneration of other tissues [32,33]. Harnessing the chondrogenic potential of ACPCs by combining them with a biomaterial matrix permissive for cartilage production, and demonstrating their use as a bio-ink for advanced biofabrication strategies, can help advance the design of more functional implants for cartilage repair and regeneration.

Therefore, the aim of this study was to evaluate the potential of ACPC-laden hydrogel constructs for cartilage regeneration and to compare their extracellular matrix (ECM) synthesis capacity with native articular chondrocytes and bone marrow-derived MSCs. A photosensitive, gelatin methacryloyl (gelMA) hydrogel bioink was used as a platform for cell encapsulation and 3D culture, and the overall production of cartilage ECM by all three cell types was assessed, together with the mechanical properties of cultured constructs. Particular attention was paid to the expression of zonal markers, in order to evaluate if different progenitor cells display different preferential zonal affinities when cultured in a 3D gelMA-based milieu. Furthermore, layered co-cultures were performed as models for multi-layered cartilage constructs. Crosstalk between the different cell types and its effect on cartilage deposition were evaluated. Finally, proof-of-concept zonal cartilage constructs were biofabricated using a 3D bioprinting set-up.

Europe PMC Funders Author Manuscripts

2 Materials and methods

2.1 Synthesis of gelMA

GelMA was synthesized from gelatin type A, obtained from porcine skin (Sigma-Aldrich, The Netherlands), as described previously [34]. Briefly, a 10% w/v solution of gelatin in PBS was reacted with 1:0.6 methacrylic anhydride (Sigma-Aldrich, The Netherlands) at 50 °C for 1 h, to achieve an 80% degree of modification of the lysine residues. Excess of methacrylic anhydride was removed by cen-trifugation. The resulting gelMA solution was neutralized with 1 M NaOH and dialyzed against distilled water. Eventually, the gelMA solution was sterile-filtered, freeze-dried and stored at -20 °C until used.

2.2 Cell isolation

All animal tissue and cells used in this study were obtained from deceased equine donors, donated to science by their owner, and according to the guidelines of the Institutional Animal Ethical Committee. These were all skeletally mature horses, aged 37 years old, not suffering from any disorder of the joints from which cartilage was harvested or from any disorder possibly affecting MSCs in case of harvesting bone marrow. Equine cells were chosen due to the morphological and biochemical similarity between human and equine cartilage tissue [35], and in the perspective of successive preclinical testing, as the equine model is important for testing cartilage repair strategies [36,37]. At the same time, horses are also patients when it comes to joint pathologies.

2.2.1 Chondrocytes and ACPCs—Macroscopically healthy cartilage from the metacarpophalangeal joint of two equine donors was harvested with a scalpel under sterile conditions, without damaging the tidemark. The tissue was minced and digested in 0.2% pronase for 2 h, followed by incubation for 12 h in a 0.075% collagenase type 2 solution. The tissue digest was sieved through a 70 μm cell strainer and the resulting single-cell suspension was centrifuged for 5 min at 300g. Pelleted chondrocytes (CH) were washed in phosphate buffered saline (PBS) and counted with a hemocytometer. An aliquot of the total cell harvest was used to isolate ACPCs, the remaining chondrocytes were stored in liquid nitrogen until further use. Prior to encapsulation in gelMA, chondrocytes were expanded to passage 1 in Dulbecco's modified Eagle medium (DMEM, 31966, Gibco, The Netherlands), supplemented with 10% v/v heat-inactivated fetal calf serum (FCS, Gibco, The Netherlands), 0.2 mM ascorbic acid-2-phosphate, 100 U/mL penicillin and 100 μg/mL streptomycin.

ACPCs were isolated as previously described [18]. Briefly, an aliquot of the freshly isolated cartilage cells was pelleted by centrifugation, suspended in serum-free DMEM, and plated in fibronectin-coated tissue culture plates, at a density of 500 cells cm^{-2}. After 20 min, non-adherent cells were removed, and the attached cells were cultured in chondroprogenitor expansion medium (DMEM, supplemented with 10% v/v FCS, 0.2 mM ascorbic acid-2-phosphate, 100 U/mL penicillin, 100 μg/mL streptomycin and 5 ng/mL basic fibroblast growth factor (bFGF, Peprotech, UK)). After 6 days, colonies with more than 32 cells were marked for cloning. Collected colonies were pooled and cells were expanded until passage 3 before being used for the study.

Europe PMC Funders Author Manuscripts

2.2.2 MSCs—Bone marrow aspirates were obtained from the sternum of two equine donors, as previously described [17]. Briefly, the mononuclear cell fraction was derived from the bone marrow aspirate in a Ficoll-paque density gradient (GE Healthcare, The Netherlands), after centrifugation for 30 min at 100g. The mononuclear cell fraction was collected, washed with PBS and centrifuged again at 300g for 10 min. Finally, the cells were plated on tissue culture plastic and cultured in MSC expansion medium, consisting of αMEM (22561 Gibco, The Netherlands) supplemented with 0.2 mM L-ascorbic acid 2-phosphate (Sigma), 10% FCS (Lonza, The Netherlands), 100 U/mL penicillin with 100 μg/mL streptomycin (Life Technologies, The Netherlands) and 1 ng/mL bFGF. Cells grown to passage 3 were used for this study.

2.3 Multipotency and characterization of progenitor cells

For osteogenic and adipogenic differentiation, ACPCs and MSCs were expanded plated in 6 well plates at a density of 2×10^5 cells/well, cultured until subconfluent, and cultured for 21 days either in osteogenic medium (alpha-MEM supplemented with 10% FCS, 100 U/ml penicillin, 100 μg/mL streptomycin, 0.2 mM L-ascorbic acid-2-phosphate, 20 mM β-glycerol phosphate, 100 nM dexamethasone, Sigma-Aldrich, The Netherlands), or adipogenic medium (αMEM supplemented with 10% v/v FCS, 100 U/mL penicillin, 100 μg/mL streptomycin, 0.01 mM indomethacin, 83mM isobutylmethylxanthine, and 1.72 μM bovine pancreas-derived insulin, Sigma-Aldrich, The Netherlands). Medium was refreshed every 3 days. At the end of the culture, samples were stained for calcified matrix (alizarin red) and for intracellular lipid vesicles (oil red O). For chondrogenic differentiation, 2.5×10^5 cells were pelleted by centrifugation in 15 mL Falcon tubes and cultured in chondrogenic medium (DMEM supplemented with 1% v/v insulin-transferrinselenous acid (ITS+ Premix, Corning, USA), 0.2 mM ascorbic acid-2-phosphate, 100 units/mL penicillin with 100 μg/mL streptomycin (Life Technologies, The Netherlands), 100 nM dexamethasone and 10 ng/ml transforming growth factor-β1 (TGF-β1)). Medium wash refreshed every 3 days. After 21 days, histological sections of the pellets were stained for sulphated glycosaminoglycans (GAG) with safranin-O.

Reverse transcription-polymerase chain reaction (RT-PCR), was used to characterize the gene expression of the cell surface markers CD13, CD29, CD31, CD44, CD45, CD49d, CD73, CD90, CD105, CD106, CD146 and CD166 in ACPCs and MSCs [38]. Hypoxanthine phosphoribosyltransferase-1 (HPRT1) was monitored as a housekeeping gene. The primer sequences are reported in the supplementary information (Table ST1). RNA isolation was performed on cells at passage 3 using the RNAeasy mini kit (Qiagen, Germany), following the instructions of the manufacturer. Isolated RNA was quantified by UV-vis spectrophotometry with a Nanodrop 2000 (Thermo Scientific, The Netherlands), and used as template for the PCR reaction. Amplification was carried out using a SuperScript®One-Step RT-PCR System with Platinum® Taq DNA Polymerase (Life Technologies, The Netherlands). The PCR products were run in agarose gel electrophoresis and stained with ethidium bromide.

2.4 Cell encapsulation in gelMA, and 3D monoculture and layered coculture

10% w/v gelMA was dissolved in PBS, supplemented with 0.1% w/v 2-hydroxy-1-[4-(2-hydroxyethoxy)phenyl]-2-methyl-1-propa none (Irgacure 2959, BASF, Germany) as a photoinitiator. The temperature of this solution was stabilized at 37 °C, prior to cell mixing. For the monoculture samples, 1.5.107 cells/mL (ACPC, MSC or CH) were homogeneously suspended in the macromer solution, and cast into a custom-made Teflon mold to produce cylindrical samples (height = 2 mm, diameter = 6 mm). The mixture was UV-irradiated for 5 min (λ = 365 nm, E = 3 mW cm^{-2} at h = 2 cm; Vilber-Lourmat 144 portable UV-lamp) to trigger the free-radical polymerization and thus the chemical crosslinking of the hydrogel. Cell-free hydrogels, prepared in the same way, were used as control.

Layered co-cultures, consisting of two adjacent hydrogels cast on top of each other, were also prepared as models for zonal constructs. In each layer only one single cell type was encapsulated, and all the possible cell combinations (ACPC/MSC, ACPC/CH and MSC/CH, all ratios 1:1) were studied. To fabricate these constructs, a gelMA macromer solution laden with the first cell type (density = 1.5-107 cells/mL) was cast into custom-made cylindrical molds (height = 2 mm, diameter = 6 mm). The mixture was partially crosslinked via UV-irradiation for 2 min, to leave unreacted methacrylate groups available for chemical binding with the second gelMA layer. Subsequently, a second mold was aligned on top of the first one, and a gelMA solution laden with the second cell type was cast. The double-layered constructs were UV-irradiated for 5 additional minutes to complete the crosslinking. No delamination was observed when handling the layered gels. An optical microscopy picture and a schematic representation of the layered 3D co-culture system are reported in the supplementary information (Fig. S1). All the samples (mono-, co-cultures and cell-free hydrogels) were cultured in chondrogenic differentiation medium as described in section 2.3.

2.5 Biochemical analysis

Samples (both monocultures and layered co-cultures) were harvested to measure DNA and sGAG content after 1, 28 and 56 days of culture (n = 4-6). The constructs were freeze-dried and digested overnight in 0.01 M cysteine, 250 μg/mL papain, 0.2 M NaH_2 PO_4 and 0.01 M EDTA at 60 °C. Subsequently, the digest sample was reacted with dimethylmethylene blue (DMMB, Sigma-Aldrich, The Netherlands), and the sGAG content calculated by determining the ratio of the absorbance at 525 and 595 nm with a spectrophotometer (Bio-Rad, Hercules, CA). Known dilutions of chondroitin sulfate were used as standards for quantitative analysis. DNA content of the constructs was quantified on papain digests, using a Quant-iT PicoGreen dsDNA kit (Life Technologies, The Netherlands).

2.6 Mechanical testing

The mechanical properties of the monoculture constructs were studied in an unconfined uniaxial compression test, with a Dynamic Mechanical Analyzer (DMA Q800, TA Instruments, The Netherlands).Samples at days 1, 28 and 56 of culture were washed with PBS and compressed at a -20%/minute strain rate (n = 4-6). The compression modulus was calculated as the slope of the stress/strain curve in the 10% to 15% strain range.

2.7 Gene expression of cartilage and zonal markers

Gene expression analysis was performed by qPCR on monoculture samples taken at days 1, 28 and 56 of culture (n=3). Constructs were harvested and mechanically ground in RLT buffer (Qiagen, Germany). The lysate was then processed with the RNeasy Mini kit to isolate mRNA. Amplification and cDNA synthesis were performed with a SuperScript III Platinum SYBR Green One-Step qRT-PCR Kit (LifeTechnologies, The Netherlands). The relative expression levels for aggrecan (ACAN), collagen type II (COL2A1), collagen type I (COL1A1), proteoglycan 4 (PRG4), collagen type X (COL10A1) and cartilage oligomeric matrix protein (COMP) were analyzed compared to the housekeeping gene HPRT1. The primers sequences are reported in the supplementary information (Table ST2). Relative expression, Ct and efficiency values were calculated using the PCRminer algorithm [39].

2.8 Histological assessment

The deposition of main constituents of the cartilage ECM in the hydrogel was assessed on formalin-fixed, paraffin-embedded samples (n = 3). Prior to the harvesting, cultured constructs were treated overnight with 0.1 μM monensin to trap PRG4 intracellularly. Tissue sections (5 μm) were sliced with a microtome and processed for the staining. sGAG content was visualized by Safranin O, collagen with fast green staining, and cell nuclei with haematoxylin. Immunohistochemistry was performed using the appropriate primary antibodies for collagen type I (sc-8784, Santa Cruz Biotechnology, USA), type II (DSHB, II-II6B3, USA) and PRG4 (ab28484, Abcam, The Netherlands). Samples were deparaffinized with xylene, hydrated in ethanol graded solutions, and treated with 0.3% v/v H_2O_2 to block endogenous peroxidases. For collagen type I and II, antigen retrieval was performed with pronase (1 mg/mL, Roche, USA) and hyaluronidase (10 mg/mL, H2126, Sigma Aldrich, The Netherlands), applied for 30 min at 37 °C. Tissue sections were blocked with bovine serum albumin (BSA, 5% w/v in PBS) for 1 h at room temperature and the primary antibody was incubated overnight at 4 °C. Depending on the primary antibody, appropriate IgGs were used as isotype controls. Sections were then incubated with a secondary antibody for 1 h at room temperature, and the staining was developed with 3,3-diaminobenzidine-horseradish peroxidase (Sigma Aldrich, The Netherlands). Cell nuclei were counterstained with hematoxylin. Sections were mounted in DPX (Millipore, USA), and micrographs were taken with an optical microscope (Olympus BX51, Olympus, Germany).

2.9 Bioprinting of zonal-like constructs

Zonal-like constructs (12 × 12 × 2.16 mm) were fabricated using a 3DDiscovery bioprinter (regenHu, Switzerland). The printer path was drawn in vector graphic and translated into g-code with the BioCAD software (regenHu, Switzerland). Three materials were loaded for printing: i) a superficial zone-mimicking bioink, consisting of 10% w/v gelMA laden with $2{\cdot}10^7$ ACPC/mL, ii) a middle/deep zone-mimicking bioink, composed of 10% w/v gelMA laden with $2{\cdot}10^7$ MSC/mL, and iii) pluronic F-127 (40% w/v in PBS) as sacrificial ink to support gelMA during the biofabrication process. Each layer was obtained printing a frame of parallel pluronic filaments (room temperature, pressure = 0.180 MPa, 23 G nozzle, translation speed=20mm/s)withastrand-to-stranddistanceof1.2mm.Sub-sequently, gelMA was dispensed in between the sacrificial strands using a microvalve (pressure = 0.04 MPa,

23 G nozzle, dosing distance = 0.3 mm, opening time = 800 μs, temperature = 37 °C, translation speed = 30 mm/s). Printed layers were pre-crosslinked for 10s via exposure to a built-in UV led (λ=365nm, E = 240.2 mW cm^{-2} at h = 1 cm). Layer height was set to 0.24 mm, and 3 D constructs with a woodlog 0°-90° structure were generated in a layer by-layer fashion. The first seven layers were printed with the MSC-laden bioink; the last two with the ACPC-laden bioink. After printing, crosslinking of gelMA was completed by exposure for 5 min to a Vilber-Lourmat 144 portable UV-lamp (λ = 365 nm, E = 3 mW cm-2 at h = 2 cm). Samples were soaked in cold PBS to remove the pluronic, cut into 3.5 × 3.5 mm squares and cultured for 56 days in chondrogenic differentiation media (n = 3). Cell viability was evaluated at day 1 and 14 after printing using calcein AM and ethidium homodimer-1 (Life Technologies) (n = 3), and compared to that of cast scaffolds. ECM deposition was qualitatively observed with histological analysis, as described in section 2.8. Morphology of the printed constructs was also observed from microscopy images and X-ray micro computerized tomography scans (λCT, Quantum FX, Perkin Elmer, USA, spatial resolution of 20 μm^3 of voxel size, scan time = 3 min, tube voltage = 90 kV and tube current = 180 μA). Additionally, a proof-of-concept fabrication of anatomically shaped constructs was performed. A computer-aided design (CAD) model of the caudal end of a human femur (maximum dimensions 26.5 × 26.3 × 23.1 mm) was processed with a CAD software (Rhinoceros, Robert McNeel and Associates, USA) to separate the distal end of the femoral condyle from the part modelling the proximal side and the underlying bone, thus generating two complementary models. The proximal part was converted to and STL file and the model was eventually printed with a digital light projection 3D printer (Ember, Autodesk, USA) using a proprietary PR48 resin (Autodesk). The height of each printed layer was set to 100 μm. Next, the distal end of the condyle was bioprinted on top of this model. A computer aided manufacturing software (CAM, BioCAM, regenHu) was used for slicing the condyle model and the g-code was generate with the BioCAD software (regenHu). The DLP-printed anatomical model was interfaced with the 3DDiscovery, and the caudal end of the condyle was printed using the approach and printing settings described above, via the co-printing of a sacrificial pluronic support and gelMA as a bioink.

2.10 Statistical analysis

Each experiment was performed in three to six replicates (n = 3-6). Quantitative results are expressed as mean ± standard deviation (SD), and the statistical analyses were performed using the GraphPad Prism 6.0 software package (GraphPad Software, USA). Comparisons between the experimental groups at different time points were performed with a two-way ANOVA, with a Bon-ferroni post hoc test. F-values and related degrees of freedom are listed in the supplementary information (Table ST3). A value of $p < 0.05$ was considered statistically significant.

3 Results

3.1 Characterization of ACPCs

Gene expression analysis showed high similarity between MSCs and ACPCs in their transcript profile of surface receptors important in defining the minimal criteria for mesenchyme stromal cell classification (Fig. 1A). Notably, much like MSCs, ACPCs were

positive for the stem cell markers CD73, CD90 and CD105, while being negative for the hematopoietic marker CD34 and for the leukocyte marker CD45 [40]. Additionally, both MSCs and ACPCs were $CD29^{+}$, $CD44^{+}$, $CD49d^{+}$, $CD106^{+}$, $CD166^{+}$, and faintly positive for CD146, $CD13^{-}$and $CD31^{-}$. ACPCs appeared to display higher expression of CD44, a cell membrane receptor for hyaluronic acid. Moreover, both bone-marrow derived MSCs and ACPCs were capable of differentiation towards osteogenic, chondrogenic and adipogenic lineage (Fig. 1B).

3.2 3D culture and chondrogenic differentiation in mono-cultures

3.2.1 Biochemical evaluation of neo-cartilage—

When cultured in 3D gelMA hydrogels, all three cell types, chondrocytes, ACPCs and MSCs were able to proliferate in the gel matrix. Significant differences in cell amount between experimental groups could be observed only at day 56, with MSC containing matrices containing less cells compared to ACPC-containing matrices, as estimated by the total DNA content of the hydrogel (Fig. 2A). As for the deposition of neo-cartilage ECM, all three cell types were able to undergo chondrogenic differentiation, and synthesized sGAGs which were retained within the hydrogel matrix. ACPCs, however outperformed articular chondrocytes both in terms of total sGAG (Fig. 2B) and sGAG normalized to DNA content (Fig. 2C), displaying values more than 2.3-fold higher than chondrocytes. On the other hand, MSCs produced significantly more sGAG than cartilage-derived cells (2.6-fold vs ACPCs and 6.3-fold vs chondrocytes).

3.2.2 Neo-tissue deposition and mechanical properties—

The compression modulus of the constructs was monitored over the culture time (Fig. 3). Cell-free gelMA samples displayed no change in the compression modulus, which remained in the range of 18-23 kPa, suggesting no significant degradation of the hydrogel in culture medium over the two months of the assay. For all the cell-laden samples, cartilage matrix synthesis and accumulation in gelMA correlated with an increase of the mechanical properties of the hydrogel. After 4 weeks, chondrocytes, ACPC and MSC-laden constructs displayed a compressive modulus ranging between 42 and 47 kPa. At 8 weeks, a further increase in stiffness was observed and a significantly higher elastic modulus was found for MSC-laden construct (≈186.8 kPa vs 101.4 kPa and 125.5 kPa of ACPCs and chondrocytes).

3.2.3 Differential mRNA expression of zonal markers in hydrogel culture—

Gene expression of cartilage-specific transcripts increased over time, confirming chondrogenic differentiation of the cells in the hydrogels (Fig. 4). In particular, aggrecan mRNA expression showed a correlation with sGAG synthesis, with higher values for MSCs 15-fold at day 28 and day 56), followed by ACPCs (≈6.6-fold at day 28 and 9.5-fold at day 56) and finally chondrocytes (4.1- and 2.1-fold at day 28 and 56 respectively;Fig. 4A). A similar behavior was found for collagen type II, with MSCs displaying about a 145-fold (day 28) and 89.3-fold (day 56) values higher than ACPCs (19-fold and 30.7-fold) and chondrocytes (5- and 2.3-fold; Fig. 4B). Collagen type I was also overexpressed in ACPCs and reached the highest values at day 28 (160.7- and 171.1-fold). In MSC-laden matrices, collagen type I showed a different trend: it was highly upregulated at the beginning of the culture (58.9-fold at day 1), increased to 81.2-fold at day 28 and decreased to a 48.1-fold

overexpression at day 56 (Fig. 4C), however this trend over the culture period was not significant. Moreover, COMP, the main non-collagenous protein in cartilage, displayed highly upregulated mRNA levels in all the experimental groups, compared to day 1 (Fig. 4D). The analysis of the superficial zone marker PRG4 showed that the gene is strongly upregulated in ACPCs (21.2- and 99.5-fold at days 28 and 56), compared to chondrocytes (15.7- and 13.2-fold) and MSCs, which displayed the lowest levels (7.1- and 6.9-fold;Fig. 4E). Conversely, collagen type X, which is a biomaker of endochondral ossification and a marker for calcified chondrocytes, was consistently downregulated in all experimental groups, but steadily increased over time in MSC-laden matrices (0.12- and 0.37-fold at day 1 and 56, respectively) and chondrocyte (0.28- to 0.48-fold), while decreasing in ACPC-laden matrices (0.35- to 0.18-fold;Fig. 4F).

3.2.4 Histological evaluation of hydrogel mono-cultures—

The presence and distribution of the main constituents of cartilage ECM in the hydrogel matrix were qualitatively observed on histological sections (Fig. 5). A clear difference in the amount of sGAGs (Fig. 5A) and collagen type II (Fig. 5B) was detected between the three cell types, correlating with the quantitative analysis for sGAGs and collagen type II gene expression. Nevertheless, all experimental groups showed the formation of interconnected, homogeneously distributed staining for sGAGs at the last time point of the culture, while only ACPCs and MSCs displayed ubiquitous staining for collagen type II. Collagen type I was also in line with what was observed in the gene expression panel, with CHs having more intense and diffused staining at earlier time points than ACPCs, and MSCs in the last place (Fig. 5C). In all experimental groups, most cells were positive for PRG4, with the least intense staining present for MSCs at 56 days of culture (Fig. 5D). Interestingly, for all the samples, a layer of spread, elongated cells, with intense and continuous PRG4 positive staining was found at the outer rim of the hydrogel.

3.3 3D co-culture in layered hydrogels

3.2.1 Biochemical analysis of layered co-cultures—

In the co-culture system, all the possible cell combinations displayed higher amounts of DNA compared to their respective monoculture controls (Fig. 6A). This effect appears to be more pronounced when MSCs are present in the construct. At days 28 and 56 MSC/chondrocyte matrices showed a 1.8- and 1.5-fold higher DNA production against monocultures, in comparison to a 1.4- and 1.5-fold increase for MSC/ACPC and a 1.3- and 1.2-fold for ACPC/chondrocyte samples, respectively. MSC/ACPC cocultured matrices displayed the highest overall sGAG concentration (≈53 μg/mg at day 28 and 136 μg/mg at day 56), followed by MSC/chondrocyte matrices (≈29 and 52 μg/mg) and ACPC/-chondrocyte matrices (≈25 and 55 μg/mg;Fig. 6B). It is worth highlighting that overall sGAG synthesis all co-culture groups, apart from MSC/chondrocyte samples, showed no significant difference with their respective mono-culture controls. As a consequence of having more cells but the same sGAG content, cocultures tended to showalowersGAG/DNAratio compared to their monoculture controls (Fig. 6C). MSC/ACPC was the best performing co-culture group (≈51 and 150 $\mu g_{GAG}/\mu g_{DNA}$ at days 28 and 56), performing better than MSC/chondrocyte (≈23 and 45 $\mu g_{sGAG}/\mu g_{DNA}$ at days 28 and 56) and ACPC/chondrocyte (≈28 and 60 μgsGAG/μgDNA at days 28 and 56).

3.3.2 Histological evaluation of layered hydrogels—Qualitative evaluation of sGAGs (Fig. 7A) and collagen type II (Fig. 7B) confirmed the trends observed in monocultures, even when cells are co-cultured in adjacent hydrogel layers, with MSCs produced more matrix, followed by ACPCs and finally chondrocytes. These differences resulted in the formation of constructs with a distinct composition in each layer. Collagen type I was homogeneously distributed throughout the hydrogel matrix (Fig. 7C), though antibody labelling was less intense compared to collagen type II labelling. PRG4 immunohistochemistry was positive intracellularly for all cells, and dense clusters of positively stained cells were found at the border of the construct, regardless of the zone of the hydrogel (Fig. 7D).

3.3.3 Bioprinted zonal-like constructs—Shape stable constructs, with zonal-like cell distribution were fabricated via bioprinting of cell-laden gelMA (Fig. 8). After photocrosslinking and removal of the sacrificial pluronic supporting frame, the materials retained their shape, no delamination was observed, and interconnected pores were present after removal of the pluronic strands (Fig. S2, Supplementary Video SV1). Cell viability was comparable between printed and cast constructs, ranging from about 75% to 90% at days 1 and 14 after fabrication (Supplementary Fig. S3). Upon long-term culture, both ACPCs and MSCs in the printed layered constructs differentiated and produced cartilage matrix, with sGAG/DNA values comparable to those found in the mono- and co-cultures (168.31 ± 51.28 $\mu g_{sGAG}/\mu g_{DNA}$, after 56 days of culture). Additionally, histological analysis confirmed a zonal difference in the distribution of sGAGs from the ACPC-laden to the MSC-laden zone. Collagen type II staining appeared more intense and homogeneous throughout the gel, compared to collagen type I, which was more intense at the border of the construct. Furthermore, anatomically-shaped models of the caudal end of a human femur condyle were successfully obtained with the proposed bioprinting approach (Fig. 9).

4 Discussion

The results of this study demonstrate the ability of adult ACPCs to synthesize neo-cartilage in a hydrogel system. ACPCs appear to have potential to replace or complement chondrocytes and MSCs that are widely established cell sources for cartilage cell-based therapies. In this study, layered cast and bioprinted constructs composed of two regions laden with distinct cell types were also produced,generatingazonal-likedistributionofthemaincartilage components.

GelMA was used as a hydrogel for cell encapsulation and printing. Overall, gelMA is becoming a widespread platform for 3D culture, organ models and tissue engineering [41], and it is also one of the most versatile bioinks for biofabrication [42–46]. Previous research already demonstrated that gelMA provides a permissive environment for neo-cartilage formation, using encapsulated chondrocytes [47,48], and MSCs [49]. In this study, all three tested cell types underwent chondrogenic differentiation and synthesized a cartilage-like matrix, which over time induced a considerable increase in the compressive properties of the hydrogel. A direct comparison can be drawn between chondrocytes and ACPCs, since these cells are obtained not only from the same donors, but also from the same tissue. More specifically, ACPCs are a subpopulation of the chondrocytes from full-thickness cartilage.

Previous studies have shown that in contrast to full-depth dedifferentiated populations of articular chondrocytes, ACPCs from the same tissue retain SOX9 gene and protein expression, and therefore differentiation capacity even after extensive culture expansion [22]. In gelMA matrices, ACPCs outperformed chondrocytes in terms of cartilage matrix production (amount and distribution of sGAGs and collagen type II, less presence of collagen type I), a difference also reflected at the level of gene expression. These results, combined with the ability of ACPCs to undergo multiple passages without losing their chondrogenic potential [18], suggest that ACPCs could be a viable alternative to chondrocytes for improving cell-based cartilage therapies (such as matrix-induced autologous chondrocyte implantation), and further investigation in this direction is warranted.

ACPCs behave similarly to MSCs in terms of *in vitro* multipotency and self-renewal. In this study, we confirmed that ACPCs display gene expression of cell surface markers that is comparable with bone marrow-derived MSCs, which is in line with previously reported data[38]. Particularly, ACPCs, being $CD34^{-}$, $CD45^{-}$, $CD73^{+}$, $CD90^{+}$, $C105^{+}$, feature the same minimal marker profile for the definition of MSCs in human tissue [40].Despite this pheno-typic similarity, marked differences were observed when chondrogenic differentiation was induced in 3D cultures. Overall, MSCs produced more sGAGs in gelMA, and displayed the highest collagen type II/type I ratio at mRNA level. Two inferences can be drawn from these data, first that the chondrogenic medium optimized for bone derived MSC differentiation may not be optimal for ACPCs, secondly that there is a lack of tissue and cell signaling found within the native stem cell niche that may be required to enable ACPCs to differentiate into more mature mid and deep zone chondrocytes[50]. Clear differences between ACPCs and MSCs were observed in terms of zonal markers. Chondrocyte hypertrophy and associated calcified cartilage production is a common concern associated with MSC use for articular cartilage repair. Though collagen type X mRNA was only weakly expressed by MSCs, possibly thanks to the continuous supply of TGF-β1 from the media, it steadily increased over time. While MSCs remain a versatile cell source for cartilage repair, ACPCs may be a better alternative to prevent inappropriate differentiation. This would be especially valuable when the chosen clinical strategy to treat cartilage defects has high risk of triggering MSC hypertrophy, for instance when osteochondral grafts which provide strong osteogenic signals in the bone component are implanted[51] Over the culture period, ACPCs showed the highest transcript expression of PRG4, a key factor in joint lubrication and a well-known superficial zone marker, and the lowest expression of collagen type X, the hallmark of calcified cartilage. This suggests that ACPCs may be primed towards a superficial zone phenotype, perhaps as a result of preconditioning due to their original niche in native cartilage. Immunohistochemistry for PRG4 showed that all three cell types were positive for this proteoglycan, especially those at the external boundary of the hydrogels. However, since the antibody stains only intracellular targets, no information was obtained on the PRG4 secreted and incorporated in the hydrogel matrix. Several researchers have attempted to enhance PRG4 expression by cultured MSCs and chondrocytes in hydrogels via mechanical stimulation [52], through the biofunctionalization of the hydrogel matrix [53], use of co-cultures [54], varying cell density and growth factors [55,56], or by directly encapsulating zonally harvested chondrocytes [57]. Instead, the utilization of ACPCs may be

a much simpler and still effective alternative for the engineering of salient features of the superficial zone.

Next, taking into consideration the differential expression of cartilage component by cells, we generated multiple combinations of bi-layered cartilage constructs. While no report is available on co-cultures involving ACPCs, MSC and chondrocytes, co-cultures have been widely described. Cell-cell contact has been identified as a key factor in enhancing GAG synthesis in MSC/chondrocytes systems [16]. At the polymer concentration used in this study, the density and stiffness of the gelMA network would limit cell migration, while mass transfer and diffusion of bioactive molecules are largely unhindered within the same gel matrix [58]. Thus, in these layered co-culture models, the only effective communication between the cells in adjacent layers is through secreted factors. As a result, the co-cultures appeared to promote cell proliferation with a consequent reduction in overall sGAG/DNA ratio. Nevertheless, consistent chondrogenic differentiation was observed, especially in the MSC/ACPC constructs and the trends detected in each layer were similar to what was found for the monocultures, with MSCs producing more sGAGs and collagen type II, followed by ACPCs and chondrocytes. This suggests the feasibility of combining ACPCs and MSCs to create zonal constructs mimicking the zonal distribution of GAGs present in native cartilage, and in recreating the cell phenotypes present during rapid growth of cartilage in immature cartilage [59].

To verify this, bioprinted layered, zonal-like constructs were created as a proof-of-concept. The superficial zone of the construct was obtained from the ACPC-laden bioink, while the middle/deep region contained MSCs. Unmodified gelMA does not exhibit a marked yield stress, and is therefore difficult to print with high shape fidelity [9,60,61]. Thus, a sacrificial pluronic frame was used to preserve the architecture of the construct during printing. This supporting role of pluronic also allowed the generation of more complex, anatomical shapes, such as the caudal end of a femoral condyle. Nevertheless, reinforcing strategies, such as the coprinting with stiffer materials will be required to provide biomechanical stability, especially in the biofabrication of large joint components [62]. ACPCs were viable after the process of printing, pluronic removal and UV crosslinking, with cell viability values comparable to those observed for MSCs undergoing the same process, showing that the process is also non-harmful for ACPCs. The mechanism of crosslinking in methacryloyl-based hydrogels has been previously demonstrated to exert a protective effect on encapsulated cells, as it utilizes the free-radicals generated by the UV irradiation [63,64]. Nevertheless, to further reduce potential concerns of UV-A light, crosslinking chemistries that require reduced UV exposure, such as thiol-ene click reactions [65], or even alternatives based on visible light [46], could be applied in the future for encapsulating ACPCs, and in general for bioprinting.

During printing, cells are subjected to a range of shear stresses, depending on the gauge and shape of the extrusion nozzle, the extrusion mechanism, the printing pressure and the bioink rheological properties. Recent studies have highlighted that above a particular shear stress threshold chondrogenic differentiation is impeded, even in absence of harmful effects on viability, especially with viscous hydrogels using a microvalve-based extrusion system [66]. The gelMA-based bio-ink, as used in this study, was also extruded through a microvalve, but

we found that higher cell functionalities like differentiation potential and cartilage matrix deposition were preserved both for ACPCs and MSCs, further demonstrating the suitability of the gel and the chosen printing set-up for cartilage bioprinting. Overall, the zonal construct showed an inhomogeneous distribution of sGAGs and collagen type II, with the concentration of these macromolecules increasing from the ACPC- to the MSC-laden zone, a zonal difference approximating the one present in native cartilage.

In mono- and co-cultured bio-inks, all cell types displayed consistent production of collagen type I alongside collagen type II, as shown in the histological and mRNA analyses. In bioprinted constructs, the higher ratio of collagen type II to type I was more evident compared to that observed for the cast hydrogels, possibly suggesting a positive effect of stresses involved in the printing process on cell differentiation. Collagen type I is physiologically present in the superficial zone of native cartilage at the articulating boundary [67], and often in repair tissue [68], but is also usually associated with a fibrocartilage phenotype. Furthermore, the lack of mechanical loading may add to the potential of fibrous tissue formation, which has previously been observed in limb development studies utilizing the chick model [69]. Previous studies using gelMA as a bioink reported a more fibrocartilage-like matrix production from MSCs [70]. Modification of the bioink may be necessary to enhance the quality of the cartilage tissue in future experiments, as cell response can be tuned modifying the microenvironment of the hydrogel [71]. For instance, gelMA could be functionalized with hyaluronic acid, which has been previously demonstrated to inhibit the synthesis of collagen type I by encapsulated chondrocytes substantially [53], and has been successfully used to promote cartilage formation in other hydrogel systems [72]. Modification of gelatin bioinks with silk was also shown to modulate and improve chondrogenesis by MSC [73], and it may be interesting to evaluate ACPC It is clear that the use of ACPCs in regenerative medicine is still in an early stage, and different biomaterials and culture conditions will have to be tested to optimize their chondrogenic potential. Mechanical conditioning has already been shown beneficial to guide ACPC differentiation [29]. Moreover, the differentiation media used in this study contain TGF-b1 as main chondrogenic factor. This recipe has been optimized for MSCs, but a different formulation may be optimal for ACPCs [26], and it is expected that as more research will be performed involving these cells from both animal and human origin, the optimal culture conditions will be identified.

Another important aspect is the biomechanical profile of the constructs. While the *in vitro* maturation greatly increased the compressive properties of the gel, these are still not matching native cartilage. The compressive stiffness of mature equine cartilage ranges between 0.8 and 1.2 MPa [74], while our values fall in the range of immature cartilage [75], and may further be improved upon maturation through mechanical conditioning. Bioprinting of ACPCs may benefit with reinforcement strategies using highly organized microfibrous meshes, *i.e.* produced by melt electrospinning writing [47]or through co-printing with reinforcing structures [6,76], which have already been previously described and demonstrated potential to approximate the behavior of native cartilage. Convergence of these biofabrication approaches may lead to a new generation of load-bearing, hydrogel-based cartilage constructs. These new strategies could be further characterized with an in-depth analysis of the biomechanical profile of cartilage constructs,*i.e.*via(nano)indentation, tensile

Europe PMC Funders Author Manuscripts

testing, shear and friction at the surface, analysis of viscoelastic properties and response to cyclic stresses. While our present study focused on the biological performance of ACPCs, in relation to MSCs and chondrocytes, it did not provide such comprehensive mechanical characterization of the engineered constructs. Alongside accurate selection of cell sources for cartilage tissue engineering, future work should consider such mechanical testing, in order to evaluate the biomimicry of the anisotropic biomechanical profile of native articular cartilage, both under compression and tension, since achieving constructs mimicking the latter is still major challenge[77,78]. In this perspective, sets of mechanical tests, that include nanoindentation and single edge notch tests, have been previously proposed to compare native cartilage to engineered hydrogel constructs[79].

Finally, a new range of opportunities will be available for ACPCs for cartilage repair. Hydrogel encapsulation can be used with complementary strategies already proposed in the biomaterials community, including the use of hydrogels mimicking the developmental processes of cartilage, zonal gradients of growth factors and cell density, and mechanical stimulation and reinforcement strategies.

5 Conclusions

ACPCs are promising sources for cartilage regenerative medicine and biofabrication, and the encapsulation in gelMA hydrogels allowed the formation of 3D cartilage constructs *in vitro*. The interplay of ACPCs with chondrocytes and MSCs supported neocartilage synthesis in layered co-cultures, indicating the possibility to use ACPCs also as a complementary cell source in cartilage constructs to produce functionally relevant differentiated tissue and to also act as a pool of stem cells for further growth and remodeling. The amount and quality of neo-cartilage matrix produced by ACPCs was superior to that generated by encapsulated expanded chondrocytes. Even though ACPC-laden hydrogels showed a lower production of ECM components compared to MSC-laden ones, ACPCs displayed distinctive phenotypic features, particularly a low expression of collagen type X and a high expression of PRG4, suggesting a priming toward a phenotype similar to superficial zone chondrocytes. When used as bioink, the ACPC-gelMA combination could be safely printed and combined with MSCs in a zonal-like architecture leading to a biomimetic GAG distribution. As the compressive mechanical properties of our hydrogel-only constructs did not reach those of adult articular cartilage, combination with reinforcement strategies or bioreactor culture will be recommended to fully address the complex mechanical behavior of cartilage under compression, but also in response to tensile and shear stresses. Consequently, future studies focusing on in-depth biomechanical characterization will play an important role in the field of cartilage tissue engineering. Importantly, further research on ACPC biology, 3D culture and bioprinting will be required to fully recapitulate the zonal organization of native cartilage. Overall, the results of this study provide important insights for the design of the next generation of cell- and biomaterial-based articular cartilage therapies.

Supplementary Material

Refer to Web version on PubMed Central for supplementary material.

Acknowledgments

The authors acknowledge Alessia Longoni and Behdad Pouran for their help with the μCT imaging. The research leading to these results has received funding from the European Community's Seventh Framework Program (FP7/2007-2013) under grant agreement 309962 (HydroZONES), the European Research Council under grant agreement 647426 (3D-JOINT), the Dutch Arthritis Foundation (LLP-12, LLP-22 and CO-14-1-001), UK Regenerative Medicine Platform (MR/L02280X/1) and Arthritis Research UK (20864).

References

[1]. Prakash D, Learmonth D. Natural progression of osteo-chondral defect in the femoral condyle. Knee. 2002; 9:7–10. DOI: 10.1016/S0968-0160(01)00133-8 [PubMed: 11830374]

[2]. Bernhard JC, Vunjak-Novakovic G. Should we use cells, biomaterials, or tissue engineering for cartilage regeneration? Stem Cell Res Ther. 2016; 7:56.doi: 10.1186/s13287-016-0314-3 [PubMed: 27089917]

[3]. Knutsen G, Drogset JO, Engebretsen L, Grøntvedt T, Isaksen V, Ludvigsen TC, Roberts S, Solheim E, Strand T, Johansen O. A randomized trial comparing autologous chondrocyte implantation with microfracture. Findings at five years. J Bone Joint Surg Am. 2007; 89:2105–2105. DOI: 10.2106/JBJS.G.00003 [PubMed: 17908884]

[4]. Yang J, Shrike Zhang Y, Yue K, Khademhosseini A. Cell-laden hydrogels for osteochondral and cartilage tissue engineering. Acta Biomater. 2017; 57:1–1. DOI: 10.1016/j.actbio.2017.01.036 [PubMed: 28088667]

[5]. Groll J, Boland T, Blunk T, Burdick JA, Cho DW, Dalton PD, Derby B, Forgacs G, Li Q, Mironov VA, Moroni L. Malda, Biofabrication: reappraising the definition of an evolving field. Biofabrication. 2016; 8:13001.doi: 10.1088/1758-5090/8/1/013001

[6]. Kang HW, Lee SJ, Ko IK, Kengla C, Yoo JJ, Atala A. A 3D bioprinting system to produce human-scale tissue constructs with structural integrity. Nat. Biotechnol. 2016; 34:312–312. DOI: 10.1038/nbt.3413 [PubMed: 26878319]

[7]. Ren X, Wang F, Chen C, Gong X, Yin L, Yang L. Engineering zonal cartilage through bioprinting collagen type II hydrogel constructs with biomimetic chondrocyte density gradient, BMC Musculoskelet. Disord. 2016; 17:301.doi: 10.1186/s12891-016-1130-8

[8]. Levato R, Visser J, Planell JA, Engel E, Malda J, Mateos-Timoneda MA. Biofabrication of tissue constructs by 3D bioprinting of cell-laden microcarriers. Biofabrication. 2014; 6:35020.doi: 10.1088/1758-5082/6/3/035020

[9]. Mouser VHM, Levato R, Bonassar LJ, DLima DD, Grande DA, Klein TJ, Saris DBF, Zenobi-Wong M, Gawlitta D, Malda J. Three-dimensional bioprinting and its potential in the field of articular cartilage regeneration. Cartilage. 2016; doi: 10.1177/1947603516665445

[10]. Cucchiarini M, Madry H, Guilak F, Saris DB, Stoddart MJ, Koon Wong M, Roughley P. A vision on the future of articular cartilage repair. Eur Cell Mater. 2014; 27:12–12. [PubMed: 24802612]

[11]. Pescosolido L, Vermonden T, Malda J, Censi R, Dhert WJA, Alhaique F, Hennink WE, Matricardi P. In situ forming IPN hydrogels of calcium alginate and dextran-HEMA for biomedical applications. Acta Biomater. 2011; 7:1627–1633. DOI: 10.1016/j.actbio.2010.11.040 [PubMed: 21130186]

[12]. Pei M, He F, Boyce BM, Kish VL. Repair of full-thickness femoral condyle cartilage defects using allogeneic synovial cell-engineered tissue constructs, Osteoarthr. Cartil. 2009; 17:714–714. DOI: 10.1016/j.joca.2008.11.017

[13]. Ha CW, Park YB, Chung JY, Park YG. Cartilage Repair Using Composites of Human Umbilical Cord Blood-Derived Mesenchymal Stem Cells and Hyaluronic Acid Hydrogel in a Minipig Model. Stem Cells Transl Med. 2015; 4:1044–1044. DOI: 10.5966/sctm.2014-0264 [PubMed: 26240434]

[14]. Guo X, Park H, Young S, Kretlow JD, van den Beucken JJ, Baggett LS, Tabata Y, Kasper FK, Mikos AG, Jansen JA. Repair of osteochondral defects with biodegradable hydrogel composites encapsulating marrow mesenchymal stem cells in a rabbit model. Acta Biomater. 2010; 6:39–39. DOI: 10.1016/j.actbio.2009.07.041 [PubMed: 19660580]

Europe PMC Funders Author Manuscripts

[15]. Park JS, Shim MS, Shim SH, Yang HN, Jeon SY, Woo DG, Lee DR, Yoon TK, Park KH. Chondrogenic potential of stem cells derived from amniotic fluid, adipose tissue, or bone marrow encapsulated in fibrin gels containing TGF-b3. Biomaterials. 2011; 32:8139–8139. DOI: 10.1016/j.biomaterials.2011.07.043 [PubMed: 21840589]

[16]. de Windt TS, Vonk LA, Slaper-Cortenbach ICM, van den Broek MPH, Nizak R, van Rijen MHP, de Weger RA, Dhert WJA, Saris DBF. Allogeneic mesenchymal stem cells stimulate cartilage regeneration and are safe for single-stage cartilage repair in humans upon mixture with recycled autologous chondrons. Stem Cells. 2016; doi: 10.1002/stem.2475

[17]. Visser J, Gawlitta D, Benders KEM, Toma SMH, Pouran B, van Weeren PR, Dhert WJA, Malda J. Endochondral bone formation in gelatin methacrylamide hydrogel with embedded cartilage-derived matrix particles. Biomaterials. 2015; 37:174–182. DOI: 10.1016/j.biomaterials.2014.10.020 [PubMed: 25453948]

[18]. Williams R, Khan IM, Richardson K, Nelson L, McCarthy HE, Analbelsi T, Singhrao SK, Dowthwaite GP, Jones RE, Baird DM, Lewis H, et al. Identification and clonal characterisation of a progenitor cell sub-population in normal human articular cartilage. PLoS One. 2010; 5doi: 10.1371/journal.pone.0013246

[19]. Alsalameh S, Amin R, Gemba T, Lotz M. Identification of mesenchymal progenitor cells in normal and osteoarthritic human articular cartilage. Arthritis Rheum. 2004; 50:1522–1522. DOI: 10.1002/art.20269 [PubMed: 15146422]

[20]. Dowthwaite GP, Bishop JC, Redman SN, Khan IM, Rooney P, Evans DJR, Haughton L, Bayram Z, Boyer S, Thomson B, Wolfe MS, Archer CW. The surface of articular cartilage contains a progenitor cell population. J Cell Sci. 2004; 117:889–889. DOI: 10.1242/jcs.00912 [PubMed: 14762107]

[21]. Jiang Y, Tuan RS. Origin and function of cartilage stem/progenitor cells in osteoarthritis. Nat Rev Rheumatol. 2015; 11:206–206. DOI: 10.1038/nrrheum.2014.200 [PubMed: 25536487]

[22]. Khan IM, Bishop JC, Gilbert S, Archer CW. Clonal chondroprogenitors maintain telomerase activity and Sox9 expression during extended monolayer culture and retain chondrogenic potential, Osteoarthr. Cartil. 2009; 17:518–528. DOI: 10.1016/j.joca.2008.08.002

[23]. Jayasuriya CT, Chen Q. Potential benefits and limitations of utilizing chondroprogenitors in cell-based cartilage therapy, Connect. Tissue Res. 2015; 56:265–265. DOI: 10.3109/03008207.2015.1040547

[24]. Studer D, Cavalli E, Formica FA, Kuhn GA, Salzmann G, Mumme M, Steinwachs MR, Laurent-Applegate LA, Maniura-Weber K, Zenobi-Wong M. Human chondroprogenitors in alginate-collagen hybrid scaffolds produce stable cartilage in vivo. J Tissue Eng Regen Med. 2016; doi: 10.1002/term.2203

[25]. Kozhemyakina E, Zhang M, Ionescu A, Ayturk UM, Ono N, Kobayashi A, Kronenberg H, Warman ML, Lassar AB. Identification of a Prg4-expressing articular cartilage progenitor cell population in mice. Arthritis Rheumatol. 2015; 67:1261–1261. DOI: 10.1002/art.39030 [PubMed: 25603997]

[26]. Khan IM, Francis L, Theobald PS, Perni S, Young RD, Prokopovich P, Conlan RS, Archer CW. In vitro growth factor-induced bio engineering of mature articular cartilage. Biomaterials. 2013; 34:1478–1478. DOI: 10.1016/j.biomaterials.2012.09.076 [PubMed: 23182922]

[27]. Fellows CR, Williams R, Davies IR, Gohil K, Baird DM, Fairclough J, Rooney P, Archer CW, Khan IM. Characterisation of a divergent progenitor cell sub-populations in human osteoarthritic cartilage: the role of telomere erosion and replicative senescence. Sci Rep. 2017; 7:41421.doi: 10.1038/srep41421 [PubMed: 28150695]

[28]. McCarthy HE, Bara JJ, Brakspear K, Singhrao SK, Archer CW. The comparison of equine articular cartilage progenitor cells and bone marrow-derived stromal cells as potential cell sources for cartilage repair in the horse. Vet J. 2012; 192:345–345. DOI: 10.1016/j.tvjl.2011.08.036 [PubMed: 21968294]

[29]. Neumann AJ, Gardner OFW, Williams R, Alini M, Archer CW, Stoddart MJ. Human articular cartilage progenitor cells are responsive to mechanical stimulation and adenoviral-mediated overexpression of bone-morphogenetic protein 2. PLoS One. 2015; 10doi: 10.1371/journal.pone.0136229

[30]. Frisbie DD, McCarthy HE, Archer CW, Barrett MF, McIlwraith CW. Evaluation of articular cartilage progenitor cells for the repair of articular defects in an equine model. J Bone Joint Surg Am. 2015; 97:484–484. DOI: 10.2106/JBJS.N.00404 [PubMed: 25788305]

[31]. Jiang Y, Cai Y, Zhang W, Yin Z, Hu C, Tong T, Lu P, Zhang S, Neculai D, Tuan RS, Ouyang HW. Human cartilage-derived progenitor cells from committed chondrocytes for efficient cartilage repair and regeneration. Stem Cells Transl Med. 2016; :499–499. DOI: 10.5966/sctm.2015-0192

[32]. Liu G, Wang X, Sun X, Deng C, Atala A, Zhang Y. The effect of urine-derived stem cells expressing VEGF loaded in collagen hydrogels on myogenesis and innervation following after subcutaneous implantation in nude mice. Biomaterials. 2013; 34:8617–8629. DOI: 10.1016/j.biomaterials.2013.07.077 [PubMed: 23932297]

[33]. Gaetani R, Feyen DAM, Verhage V, Slaats R, Messina E, Christman KL, Giacomello A, Doevendans PAFM, Sluijter JPG. Epicardial application of cardiac progenitor cells in a 3D-printed gelatin/hyaluronic acid patch preserves cardiac function after myocardial infarction. Biomaterials. 2015; 61:339–339. DOI: 10.1016/j.biomaterials.2015.05.005 [PubMed: 26043062]

[34]. Melchels FPW, Dhert WJA, Hutmacher DW, Malda J. Development and characterisation of a new bioink for additive tissue manufacturing. J Mater Chem B. 2014; 2:2282.doi: 10.1039/c3tb21280g [PubMed: 32261716]

[35]. Malda J, Benders KEM, Klein TJ, de Grauw JC, Kik MJL, Hutmacher DW, Saris DBF, van Weeren PR, Dhert WJA. Comparative study of depth-dependent characteristics of equine and human osteochondral tissue from the medial and lateral femoral condyles, Osteoarthr. Cartil. 2012; 20:1147–1147. DOI: 10.1016/j.joca.2012.06.005

[36]. Hurtig MB, Buschmann MD, Fortier LA, Hoemann CD, Hunziker EB, Jurvelin JS, Mainil-Varlet P, McIlwraith CW, Sah RL, Whiteside RA. Preclinical studies for cartilage repair: recommendations from the international cartilage repair society. Cartilage. 2011; 2:137–137. DOI: 10.1177/1947603511401905 [PubMed: 26069576]

[37]. McGowan KB, Stiegman G. Regulatory challenges for cartilage repair technologies. Cartilage. 2013; 4:4–4. DOI: 10.1177/1947603512460756 [PubMed: 26069647]

[38]. Ranera B, Lyahyai J, Romero A, Vázquez FJ, Remacha AR, Bernal ML, Zaragoza P, Rodellar C, Martín-Burriel I. Immunophenotype and gene expression profiles of cell surface markers of mesenchymal stem cells derived from equine bone marrow and adipose tissue. Vet Immunol Immunopathol. 2011; 144:147–154. DOI: 10.1016/j.vetimm.2011.06.033 [PubMed: 21782255]

[39]. Zhao S, Fernald RD. Comprehensive algorithm for quantitative real-time polymerase chain reaction. J Comput Biol. 2005; 12:1047–1047. DOI: 10.1089/cmb.2005.12.1047 [PubMed: 16241897]

[40]. Dominici M, Le Blanc K, Mueller I, Slaper-Cortenbach I, Marini F, Krause D, Deans R, Keating A, Prockop D, Horwitz E. Minimal criteria for defining multipotent mesenchymal stromal cells. The International Society for Cellular Therapy position statement. Cytotherapy. 2006; 8:315–315. DOI: 10.1080/14653240600855905 [PubMed: 16923606]

[41]. Klotz BJ, Gawlitta D, Rosenberg AJWP, Malda J, Melchels FPW. Gelatin-methacryloyl hydrogels: towards biofabrication-based tissue repair. Trends Biotechnol. 2016; 34:394–407. DOI: 10.1016/j.tibtech.2016.01.002 [PubMed: 26867787]

[42]. Mouser, Melchels FPW, Visser J, Dhert WJA, Gawlitta D, Malda J. Yield stress determines bioprintability of hydrogels based on gelatin-methacryloyl and gellan gum for cartilage bioprinting. Biofabrication. 2016; 8:35003.doi: 10.1088/1758-5090/8/3/035003

[43]. Loessner D, Meinert C, Kaemmerer E, Martine LC, Yue K, Levett PA, Klein TJ, Melchels FPW, Khademhosseini A, Hutmacher DW. Functionalization, preparation and use of cell-laden gelatin methacryloyl-based hydrogels as modular tissue culture platforms. Nat Protoc. 2016; 11:727–727. DOI: 10.1038/nprot.2016.037 [PubMed: 26985572]

[44]. Kolesky DB, Truby RL, Gladman AS, Busbee TA, Homan KA, Lewis JA. 3D bioprinting of vascularized, heterogeneous cell-laden tissue constructs. Adv Mater. 2014; 26:3124–3124. DOI: 10.1002/adma.201305506 [PubMed: 24550124]

[45]. Bhise NS, Manoharan V, Massa S, Tamayol A, Ghaderi M, Miscuglio M, Lang Q, Shrike Zhang Y, Shin SR, Calzone G, Annabi N, Shupe TD, Bishop CE, Atala A, Dokmeci MR, Khademhosseini A. A liver-on-a-chip platform with bioprinted hepatic spheroids. Biofabrication. 2016; 8:14101.doi: 10.1088/1758-5090/8/1/014101

[46]. Lim KS, Schon BS, Mekhileri NV, Brown GCJ, Chia CM, Prabakar S, Hooper GJ, Woodfield TBF. New visible-light photoinitiating system for improved print fidelity in gelatin-based bioinks. ACS Biomater Sci. Eng. 2016; 2:1752–1752. DOI: 10.1021/acsbiomaterials.6b00149

[47]. Visser J, Melchels FPW, Jeon JE, van Bussel EM, Kimpton LS, Byrne HM, Dhert WJA, Dalton PD, Hutmacher DW, Malda J. Reinforcement of hydrogels using three-dimensionally printed microfibres. Nat Commun. 2015; 6:6933.doi: 10.1038/ncomms7933 [PubMed: 25917746]

[48]. Boere KWM, Visser J, Seyednejad H, Rahimian S, Gawlitta D, Van Steenbergen MJ, Dhert WJA, Hennink WE, Vermonden T, Malda J. Covalent attachment of a three-dimensionally printed thermoplast to a gelatin hydrogel for mechanically enhanced cartilage constructs. Acta Biomater. 2014; 10:2602–2602. DOI: 10.1016/j.actbio.2014.02.041 [PubMed: 24590160]

[49]. Rothrauff BB, Shimomura K, Gottardi R, Alexander PG, Tuan RS. Anatomical region-dependent enhancement of 3-dimensional chondrogenic differentiation of human mesenchymal stem cells by soluble meniscus extracellular matrix. Acta Biomater. 2017; 49:140–140. DOI: 10.1016/j.actbio.2016.11.046 [PubMed: 27876676]

[50]. Hayes AJ, Tudor D, Nowell MA, Caterson B, Hughes CE. Chondroitin sulfate sulfation motifs as putative biomarkers for isolation of articular cartilage progenitor cells. J Histochem Cytochem. 2008; 56:125–125. DOI: 10.1369/jhc.7A7320.2007 [PubMed: 17938280]

[51]. Chen S, Fu P, Cong R, Wu HS, Pei M. Strategies to minimize hypertrophy in cartilage engineering and regeneration. Genes Dis. 2015; 2:76–76. DOI: 10.1016/j.gendis.2014.12.003 [PubMed: 26000333]

[52]. Thorpe SD, Nagel T, Carroll SF, Kelly DJ. Modulating gradients in regulatory signals within mesenchymal stem cell seeded hydrogels: a novel strategy to engineer zonal articular cartilage. PLoS One. 2013; 8doi: 10.1371/journal.pone.0060764

[53]. Levett PA, Melchels FPW, Schrobback K, Hutmacher DW, Malda J, Klein TJ. A biomimetic extracellular matrix for cartilage tissue engineering centered on photocurable gelatin, hyaluronic acid and chondroitin sulfate. Acta Biomater. 2014; 10:214–223. DOI: 10.1016/j.actbio.2013.10.005 [PubMed: 24140603]

[54]. Coates EE, Fisher JP. Engineering superficial zone chondrocytes from mesenchymal stem cells Tissue. Eng Part C Methods. 2014; 20:630–630. DOI: 10.1089/ten.TEC.2013.0224

[55]. Moeinzadeh S, Pajoum Shariati SR, Jabbari E. Comparative effect of physicomechanical and biomolecular cues on zone-specific chondrogenic differentiation of mesenchymal stem cells. Biomaterials. 2016; 92:57–57. DOI: 10.1016/j.biomaterials.2016.03.034 [PubMed: 27038568]

[56]. Bhumiratana S, Vunjak-Novakovic G. Engineering physiologically stiff and stratified human cartilage by fusing condensed mesenchymal stem cells. Methods. 2015; 84:109–109. DOI: 10.1016/j.ymeth.2015.03.016 [PubMed: 25828645]

[57]. Schuurman W, Gawlitta D, Klein TJ, ten Hoope W, van Rijen MHP, Dhert WJA, van Weeren PR, Malda J. Zonal chondrocyte subpopulations reacquire zone-specific characteristics during *in vitro* redifferentiation, Am. J Sports Med. 2009; 37:97S–104S. DOI: 10.1177/0363546509350978

[58]. Nichol JW, Koshy ST, Bae H, Hwang CM, Yamanlar S, Khademhosseini A. Cell-laden microengineered gelatin methacrylate hydrogels. Biomaterials. 2010; 31:5536–5536. DOI: 10.1016/j.biomaterials.2010.03.064 [PubMed: 20417964]

[59]. Hunziker EB, Kapfinger E, Geiss J. The structural architecture of adult mammalian articular cartilage evolves by a synchronized process of tissue resorption and neoformation during postnatal development, Osteoarthr. Cartil. 2007; 15:403–403. DOI: 10.1016/j.joca.2006.09.010

[60]. Billiet T, Gevaert E, De Schryver T, Cornelissen M, Dubruel P. The 3D printing of gelatin methacrylamide cell-laden tissue-engineered constructs with high cell viability. Biomaterials. 2014; 35:49–49. DOI: 10.1016/j.biomaterials.2013.09.078 [PubMed: 24112804]

[61]. Suntornnond R, An J, Chua CK. Roles of support materials in 3D bioprinting. Int J Bioprinting. 2017; 3:83–83. DOI: 10.18063/IJB.2017.01.006

[62]. Groen WM, Diloksumpan P, van Weeren PR, Levato R, Malda J. From intricate to integrated: Biofabrication of articulating joints. J Orthop Res. 2017; doi: 10.1002/jor.23602

[63]. Fedorovich NE, Oudshoorn MH, van Geemen D, Hennink WE, Alblas J, Dhert WJA. The effect of photopolymerization on stem cells embedded in hydrogels. Biomaterials. 302009; :344–344. DOI: 10.1016/j.biomaterials.2008.09.037 [PubMed: 18930540]

[64]. Bartnikowski M, Bartnikowski NJ, Woodruff MA, Schrobback K, Klein TJ. Protective effects of reactive functional groups on chondrocytes in photocrosslinkable hydrogel systems. Acta Biomater. 2015; 27:66–66. DOI: 10.1016/j.actbio.2015.08.038 [PubMed: 26318806]

[65]. Stichler S, Jungst T, Schamel M, Zilkowski I, Kuhlmann M, Bock T, Blunk T, Tessmar J, Groll J. Thiol-ene Clickable Poly(glycidol) Hydrogels for Biofabrication. Ann Biomed Eng. 2017; 45:273–273. DOI: 10.1007/s10439-016-1633-3 [PubMed: 27177637]

[66]. Müller M, Öztürk E, Arlov Ø, Gatenholm P, Zenobi-Wong M. Alginate sulfate-nanocellulose bioinks for cartilage bioprinting applications. Ann Biomed Eng. 2016; :1–1. DOI: 10.1007/s10439-016-1704-5 [PubMed: 26620776]

[67]. Hayes AJ, Hall A, Brown L, Tubo R, Caterson B. Macromolecular organization and in vitro growth characteristics of scaffold-free neocartilage grafts. J Histochem Cytochem. 2007; 55:853–853. DOI: 10.1369/jhc.7A7210.2007 [PubMed: 17478447]

[68]. Hoemann CD, Tran-Khanh N, Chevrier A, Chen G, Lascau-Coman V, Mathieu C, Changoor A, Yaroshinsky A, McCormack RG, Stanish WD, Buschmann MD. Chondroinduction is the main cartilage repair response to microfracture and microfracture with BST-cargel. Am J Sports Med. 2015; 43:2469–2469. DOI: 10.1177/0363546515593943 [PubMed: 26260465]

[69]. Roddy KA, Prendergast PJ, Murphy P. Mechanical influences on morphogenesis of the knee joint revealed through morphological, molecular and computational analysis of immobilised embryos. PLoS One. 2011; 6doi: 10.1371/journal.pone.0017526

[70]. Daly AC, Critchley SE, Rencsok EM, Kelly DJ. A comparison of different bioinks for 3D bioprinting of fibrocartilage and hyaline cartilage. Biofabrication. 82016; :45002.doi: 10.1088/1758-5090/8/4/045002

[71]. Lee JM, Yeong WY. Design and Printing Strategies in 3D Bioprinting of Cell-Hydrogels: A Review, Adv. Healthcare Mater. 2016; 5:2856–2856. DOI: 10.1002/adhm.201600435

[72]. H. Search, C. Journals, A. Contact, M. Iopscience, I.P. Address, A.M. Keyser, T.A. Manuscript, I.O.P. Publishing, C.C. By, A. Manuscript, C.C. By, A. Manuscript, Ce Pte Us Pt, 2017.

[73]. Chawla S, Kumar A, Admane P, Bandyopadhyay A, Ghosh S. Elucidating role of Silk-gelatin bioink to recapitulate articular cartilage differentiation in 3D bioprinted constructs. Bioprinting. 2017; doi: 10.1016/j.bprint.2017.05.001

[74]. Griffin DJ, Bonnevie ED, Lachowsky DJ, Hart JCA, Sparks HD, Moran N, Matthews G, Nixon AJ, Cohen I, Bonassar LJ. Mechanical characterization of matrix-induced autologous chondrocyte implantation (MACI) grafts in an equine model at 53 weeks. J Biomechnol. 2015; 48:1944–1944. DOI: 10.1016/j.jbiomech.2015.04.010

[75]. Balcom NT, Berg-Johansen B, Dills KJ, Van Donk JR, Williams GM, Chen AC, Hazelwood SJ, Sah RL, Klisch SM. In vitro articular cartilage growth with sequential application of IGF-1 and TGF-b1 enhances volumetric growth and maintains compressive properties. J Biomech Eng. 2012; 134:31001.doi: 10.1115/1.4005851

[76]. Melchels FPW, Blokzijl MM, Levato R, Peiffer QC, de Ruijter M, Hennink WE, Vermonden T, Malda J. Hydrogel-based reinforcement of 3D bioprinted constructs. Biofabrication. 82016; :35004.doi: 10.1088/1758-5090/8/3/035004

[77]. Lee JK, Huwe LW, Paschos N, Aryaei A, Gegg CA, Hu JC, Athanasiou KA. Tension stimulation drives tissue formation in scaffold-free systems. Nat Mater. 2017; doi: 10.1038/nmat4917

[78]. Paschos NK, Lim N, Hu JC, Athanasiou KA. Functional properties of native and tissue-engineered cartilage toward understanding the pathogenesis of chondral lesions at the knee: a bovine cadaveric study. J Orthop Res. 2017; doi: 10.1002/jor.23558

[79]. Xiao Y, Friis EA, Gehrke SH, Detamore MS. Mechanical testing of hydrogels in cartilage tissue engineering : beyond the compressive modulus. Tissue Eng Part B 19. 2013; doi: 10.1089/ten.teb.2012.0461

Europe PMC Funders Author Manuscripts

Statement of Significance

Despite its limited ability to repair, articular cartilage harbors an endogenous population of progenitor cells (ACPCs), that to date, received limited attention in biomaterials and tissue engineering applications. Harnessing the potential of these cells in 3D hydrogels can open new avenues for biomaterial-based regenerative therapies, especially with advanced biofabrication technologies (*e.g.* bioprinting). This study highlights the potential of ACPCs to generate neo-cartilage in a gelatin-based hydrogel and bioink. The ACPC-laden hydrogel is a suitable substrate for chondrogenesis and data shows it has a bias in directing cells towards a superficial zone phenotype. For the first time, ACPC-hydrogels are evaluated both as alternative for and in combination with chondrocytes and MSCs, using co-cultures and bioprinting for cartilage regeneration *in vitro*. This study provides important cues on ACPCs, indicating they represent a promising cell source for the next generation of cartilage constructs with increased biomimicry.

Europe PMC Funders Author Manuscripts

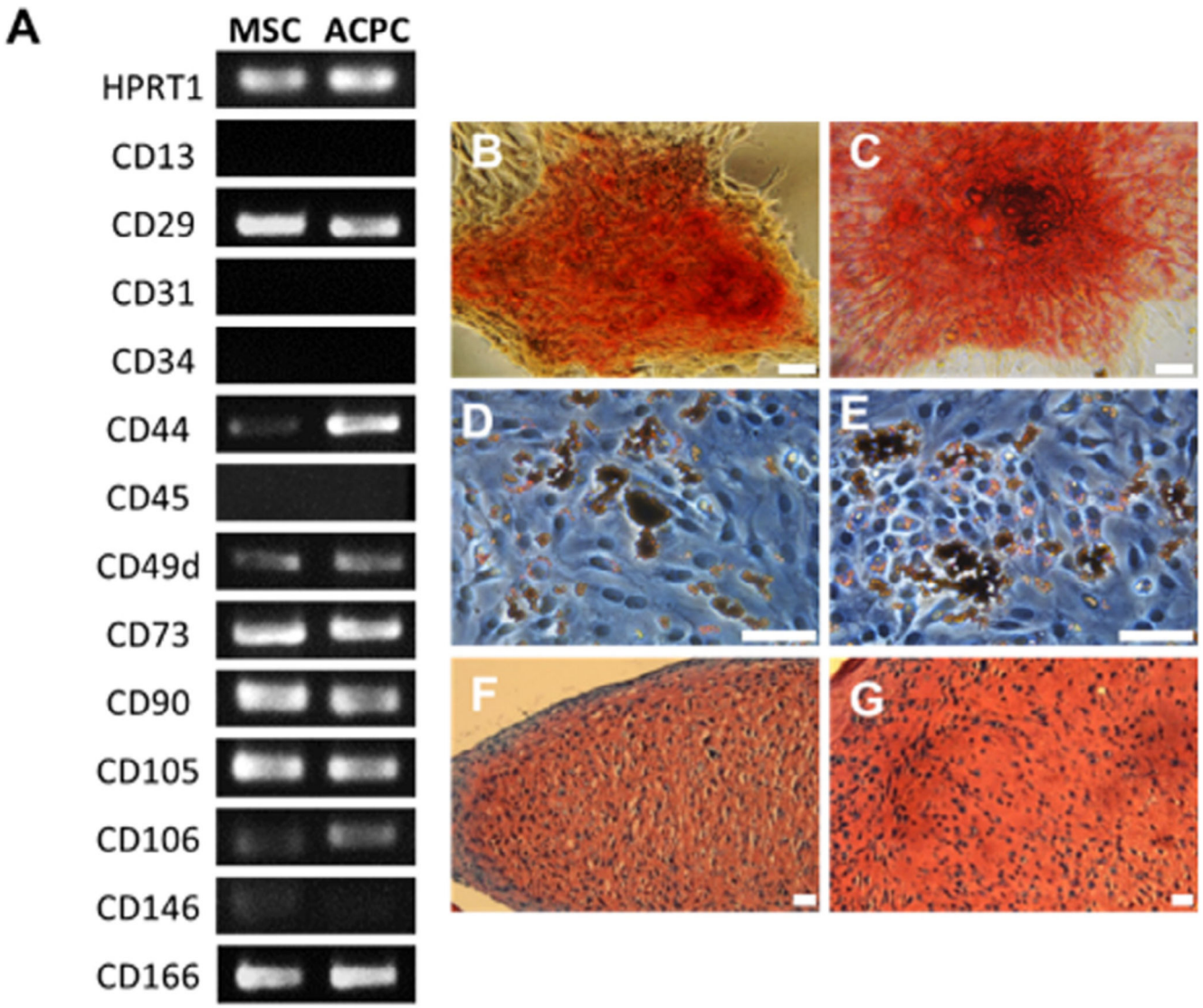

Fig. 1.

(A) Comparison of ACPC and MSC gene expression for several surface markers, as obtained from RT-PCR. Tri-lineage differentiation of (B, D, F) MSCs and (C, E, G) ACPCs, showing osteogenic (B, C, alizarin red staining), adipogenic (D, E, oil red O staining) and chondrogenic differentiation (F, G, Safranin O staining). Scale bars represent 50 μm.

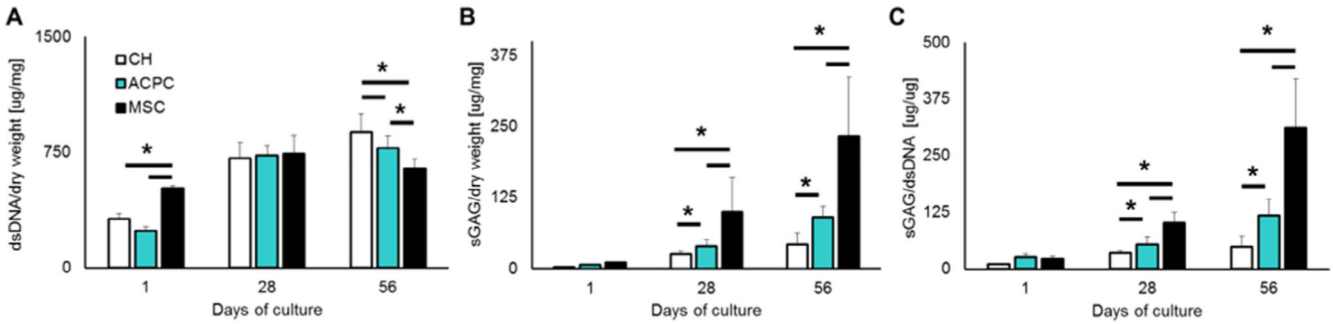

Fig. 2.

Quantification of (A) DNA and (B) sGAGs in the hydrogels for each cell type. Panel (C) shows sGAGs normalized per DNA content. ACPCs outperformed chondrocytes, while MSCs showed the highest sGAG/DNA ratio among the three cell types tested.

Europe PMC Funders Author Manuscripts

Europe PMC Funders Author Manuscripts

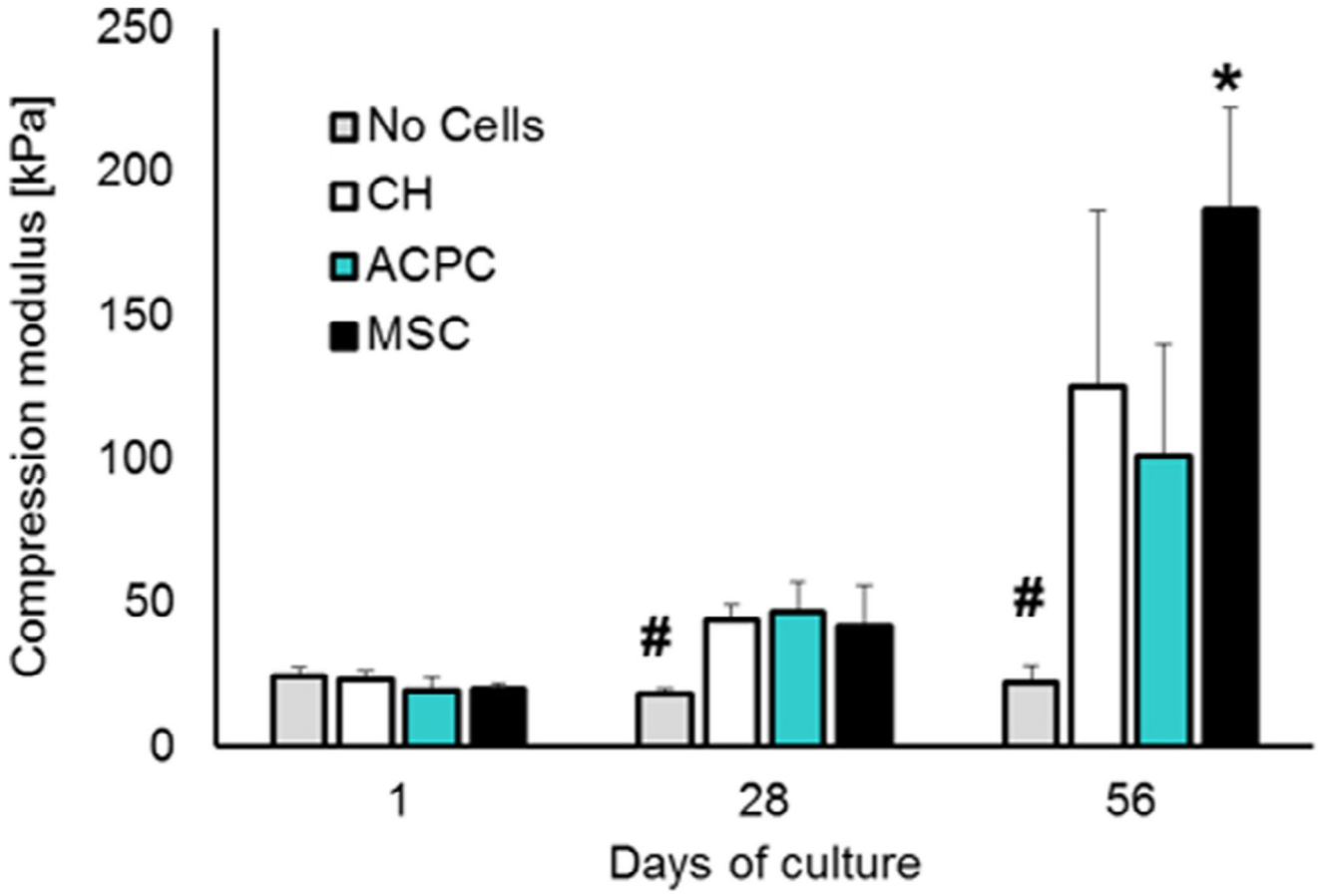

Fig. 3.

Compression modulus of cell-laden hydrogels along the culture period. * and # denote significant differences compared to all the other experimental groups ($p < 0.05$).

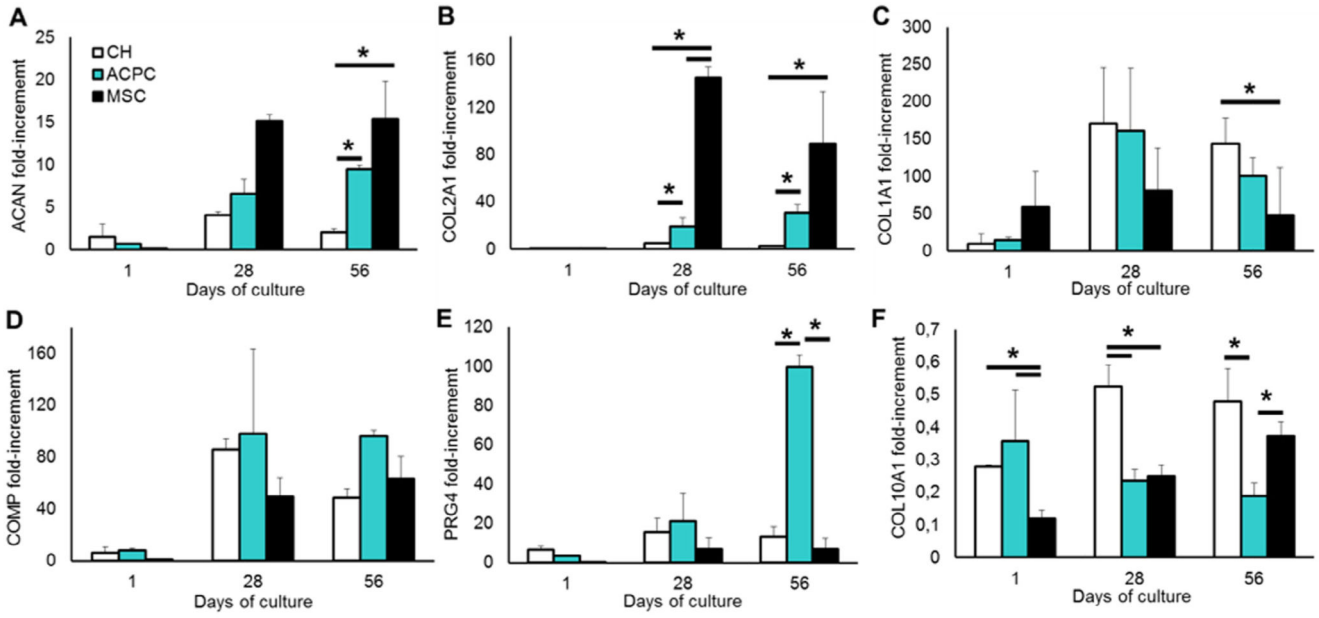

Fig. 4.

qPCR analysis of the cell-laden hydrogels, showing relative gene expression of (A) aggrecan, (B) collagentypeII, (C) collagen type I,(D)COMP,(E)PRG4 and (F)collagen type X, normalized against the housekeeping gene HPRT1. Statistically significant differences are marked with an * ($p < 0.05$).

Europe PMC Funders Author Manuscripts

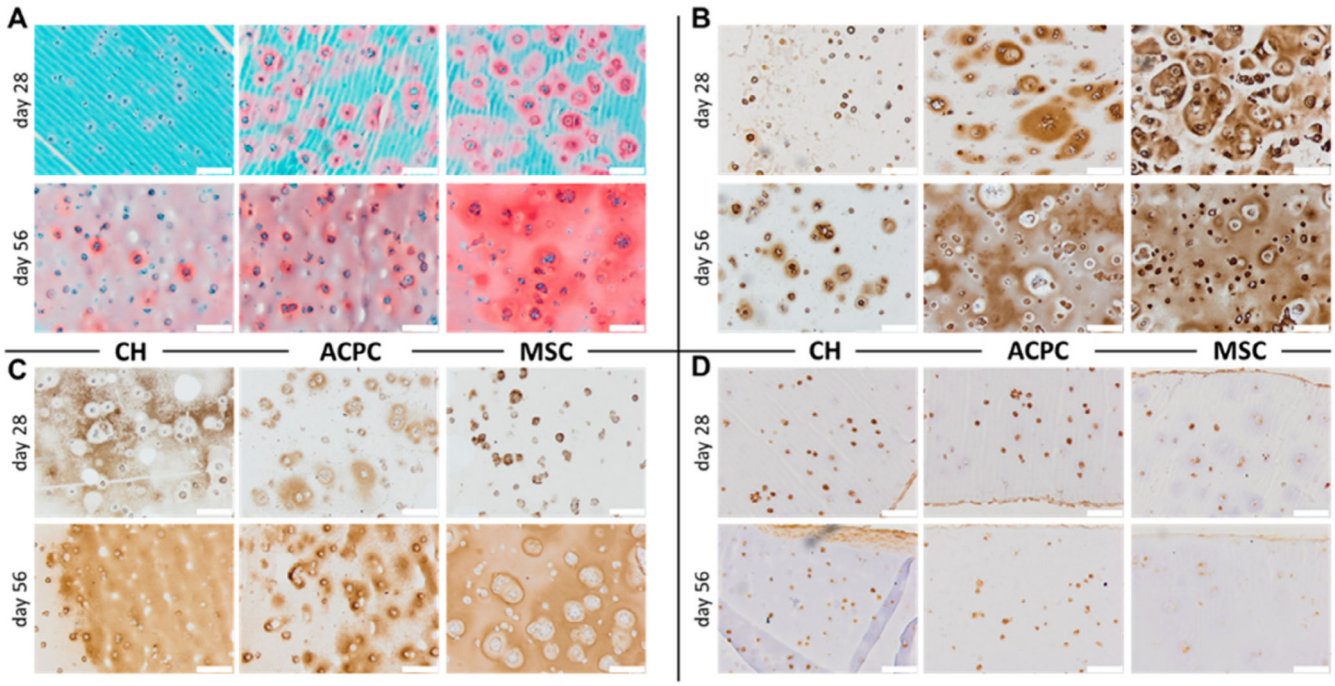

Fig. 5.

Histological analysis of the cultures at days 28 and 56. (A) Safranin O staining, and immunohistochemistry for (B) collagen type II, (C) collagen type I, and (D) PRG4. Scale bar is 200 μm.

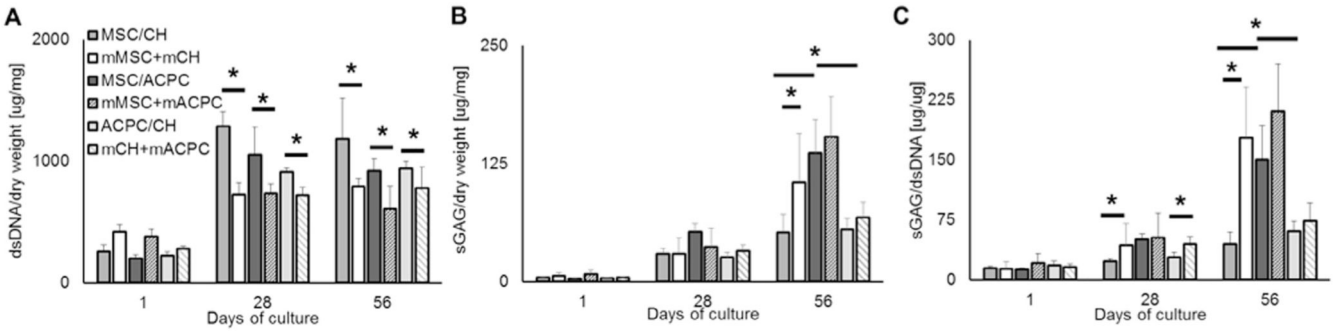

Fig. 6.

Biochemical analysis of the layered co-cultures, showing quantification of (A) DNA, (B) sGAGs, and (C) sGAGs normalized to DNA content. Statistically significant difference among the samples are indicated by an * ($p < 0.05$).

Europe PMC Funders Author Manuscripts

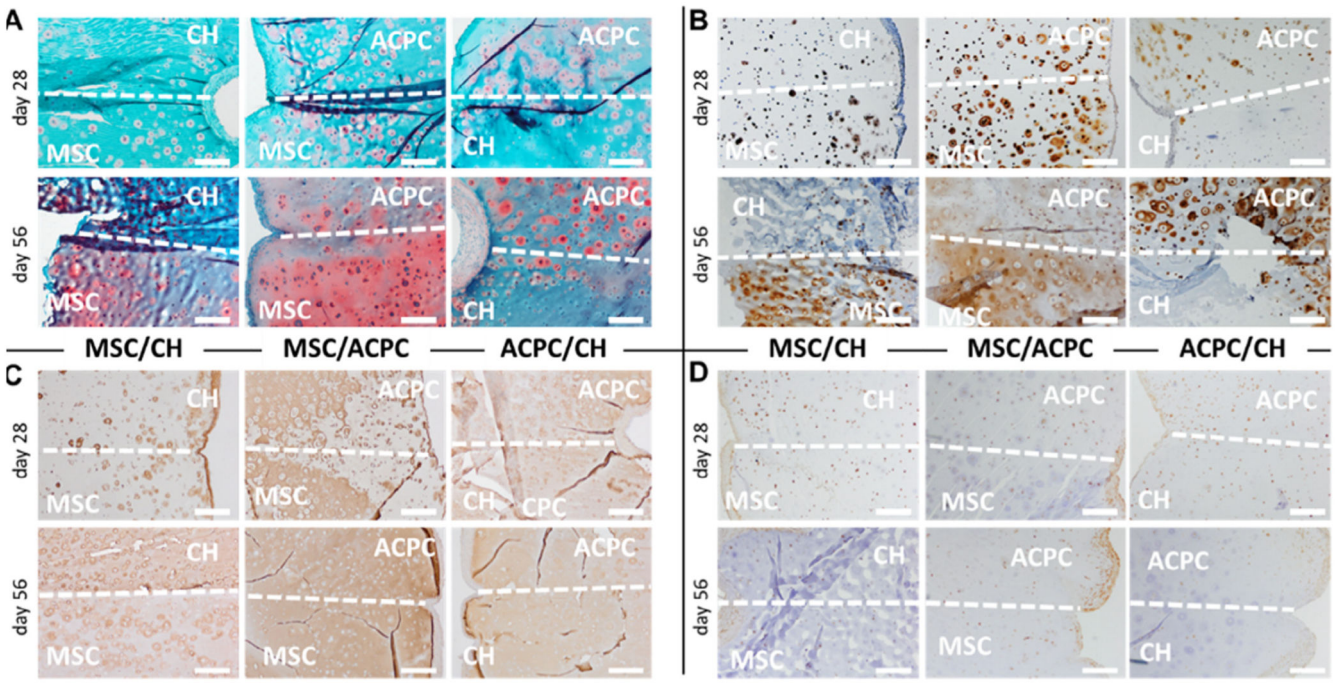

Fig. 7.

Histological sections of the layered co-cultures showing (A) safranin O staining for sGAGs, (B) collagen type II, (C) collagen type I, and (D) PRG4. The dotted line marks the interface between the two different cell-laden layers of the hydrogels, and the cell type residing in each zone is specified in overlay. Scale bar is 500 μm.

Europe PMC Funders Author Manuscripts

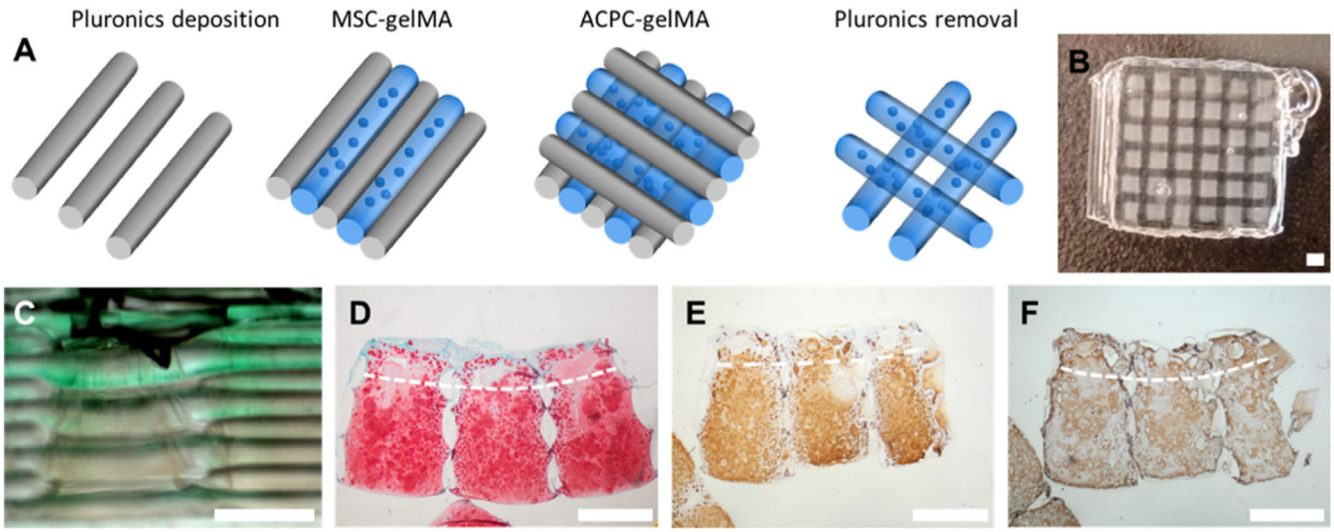

Fig. 8.

Bioprinted cartilage constructs with MSCs in the middle/deep layer and ACPCs in the superficial layer. (A) Scheme of the printing process, (B) view of the construct after printing with the pluronic frame, (C) lateral view of the construct, showing in green the superficial layer bioink. Histological staining after 56 days of culture for (D) sGAGs, (E) collagen type II, (F) collagen type 1. The dotted line indicates the border between the ACPC-laden (top) and MSC-laden (bottom) zone. Scale bar represents 1 mm.

Europe PMC Funders Author Manuscripts

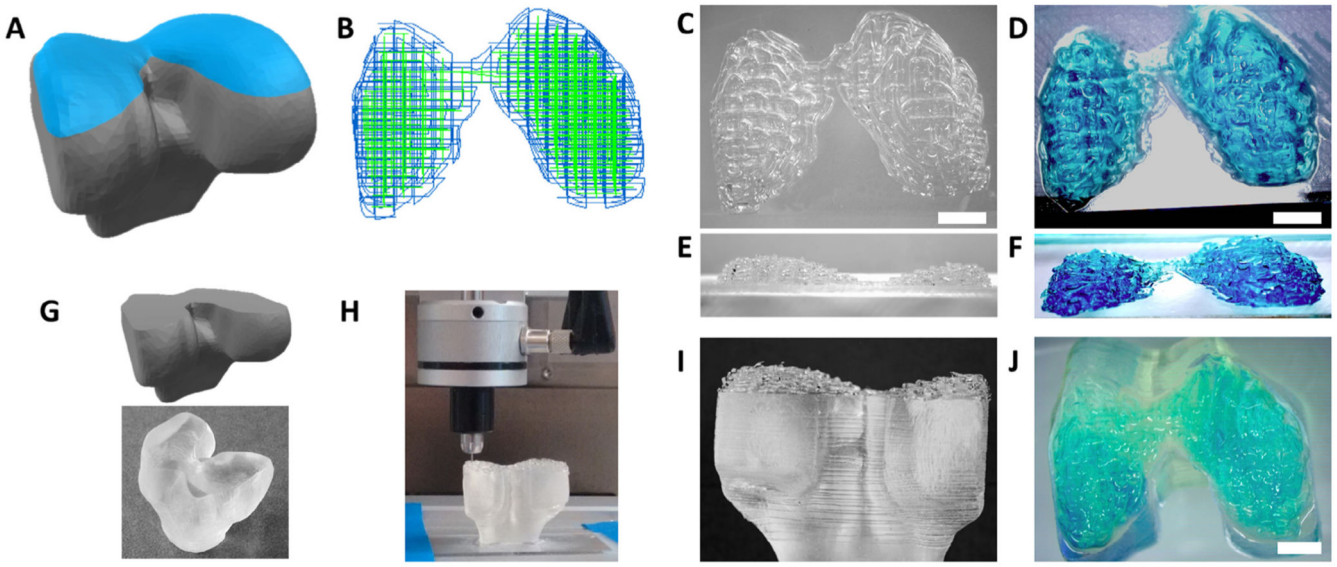

Fig. 9.

Proof-of-concept of bioprinting anatomical structures. (A) A CAD model of a femur condyle is obtained (highlighted in blue) and (B) used to generate the G-code and the path of the dual printing system (showing in blue the path for the supporting material and in green that of the bioink). (C, E) The top part of the femur condyle is printed together with the supporting hydrogel, (D,F) that can be then removed leaving only the bioink(stainedinblue).(G)A model of the lower part of the joint and the under lying bone was produced using a DLP 3D printer and (H)the condyle structure was printed directly on top of it, as a proof-of-concept test to replace the missing an atomical part, via co-extrusion of the supporting sacrificial poloxamer and gelMA bioink. (I) This allows accurate printing of the shape both in presence of the supporting material and (J) after its removal. Scale bar is 5 mm. (For interpretation of the references to colour in this figure legend, the reader is referred to the web version of this article.)

Europe PMC Funders Author Manuscripts